Available online at www.sciencedirect.com

ScienceDirect

Physics Procedia 10 (2010) 125–131

Physics Procedia

www.elsevier.com/locate/procedia

3rd International Symposium on Shape Memory Materials for Smart Systems

Mechanical cycling effects at Fe-Mn-Si-Cr-Ni SMAs obtained by powder metallurgy

B. Pricop[a], U. Söyler[b], R. I. Comăneci[a], B. Özkal[b], L. G. Bujoreanu[a,] *

[a] Faculty of Materials Science and Engineering, The "Gh. Asachi" Technical University from Iaşi, Bd. D. Mangeron 61A, 700050 Iaşi, Romania
[b] Particulate Materials Laboratory, Metallurgical and Materials Engineering Department, Istanbul Technical University, 34469 Maslak, Istanbul, Turkey

Abstract

Specimens from Fe-Mn-Si-Cr-Ni SMA, obtained by powder metallurgy and compacted through hot rolling, were subjected to tensile loading-unloading cycles. The pseudoelastic parameters were determined based on recorded stress-strain curves, and their variation tendency with increasing the number of mechanical cycles was discussed. The gauges of tensile specimens were cut after mechanical cycling and were subjected to structural and dilatometric analysis. The structure was analyzed by XRD and SEM, aiming to reveal mechanical cycling effects. The thermomechanical response on heating, of mechanically cycled specimens, was recorded by dilatometry and revealed a tendency to enhance thermal expansion as an effect of increasing the number of cycles. The microstructural changes, induced by mechanical cycling, consisted in the stress induced formation of α' martensite.

Keywords: Shape memory alloys; Powder metallurgy; Tensile testing; Mechanical cycling; Stress-induced martensite

1. Introduction

In recent years Fe-Mn-Si based shape memory alloys (SMAs), became commercially available for constrained recovery [1] applications such as pipe joints [2] and fishplates for crane rail connections [3], under the form of: Fe-28 Mn-6 Si-5 Cr [4] and Fe-14 Mn-5 Si-9 Cr-5 Ni [5], (mass. %, as all compositions will be listed hereinafter). In Fe-Mn-Si based SMAs the occurrence of shape memory effect (SME) relays on the stress induced formation of ε (hexagonal close packed, hcp) martensite on deformation and on its thermally induced reversion to γ (face centre cubic, fcc) austenite, on heating [6]. Besides ε (hcp), α' (body centre cubic, bcc) ferromagnetic martensite is stress induced at low Mn content or at high deformation degrees [7] but its presence is undesirable from the point of view of transformation reversibility [8].

In spite of the general opinion that Fe-Mn-Si based SMAs are useful as long as their manufacturing costs are less

* Corresponding author. Tel.: +40-727-486406; fax: +40-232-225986.
E-mail address: lgbujor@tuiasi.ro.

1875-3892
doi:10.1016/j.phpro.2010.11.087

than those of other proficient SMAs (such as Ni-Ti), which can be only achieved by classical metallurgy comprising ingot obtainment by means of melting, alloying and casting, a previous report has shown that thermally induced reversion of stress induced martensite occurred in slightly pre-strained specimens of powder metallurgy (PM) – manufactured Fe-Mn-Si-Cr-Ni [9]. As a continuation of that first report, the present paper aims to discuss more results obtained on a PM Fe-Mn-Si-Cr-Ni, concerning manufacturing effects and macro- and microstructural changes induced by mechanical cycling.

2. Experimental details

An Fe-18Mn-3Si-7Cr-4Ni SMA was produced by PM technology comprising pressing and sintering at 1390 K, under cracked ammonia (75 % N_2 + 25 % H_2). The specimens were produced from, commercial powders with zinc stearate binder (alloy designated as PM-Zn) and from mechanically alloyed (MA) powders, without binder (alloy designated as PM-MA). In order to increase chemical homogeneity and compactness, homogenization annealing (1370K/ 1 hr./ water) and hot-rolling 1270 K to 1mm thickness were applied. By spark erosion, specimens were cut according to the shapes shown in Fig.1.

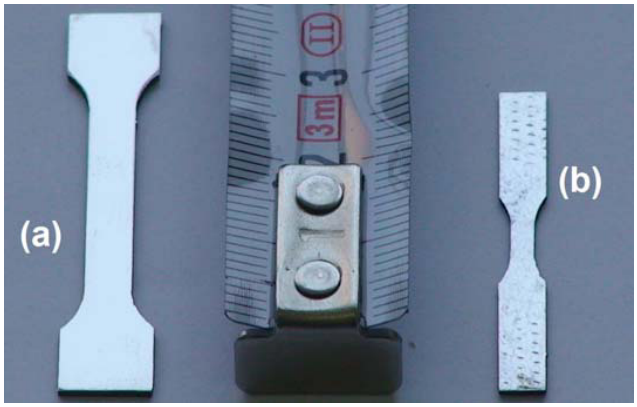

Fig.1 Specimen shapes cut by spark erosion: (a) PM-MA; (b) PM-Zn

The specimens were analyzed by tensile testing, dilatometry, X-ray diffraction (XRD) and scanning electron microscopy (SEM). Tensile loading-unloading tests were performed on an INSTRON 3382 tensile testing machine with a deformation rate of 2.77×10^{-4} sec^{-1}. Dilatometric measurements were carried out on a NETZSCH DIL 402 CD dilatometer, at a heating rate of 8.33 x 10^{-2} K/s up to 870 K, under He atmosphere, using fused silica and alumina as sample holder material and standard calibration material, respectively. XRD patterns were recorded on a BRUKER AXS D8 Advance diffractometer with Cu K_α and EVA software. SEM observations were done on a SEM – VEGA II LSH TESCAN scanning electron microscope, coupled with an EDX – QUANTAX QX2 ROENTEC detector and on a FEI Quanta 200 3D dual beam device.

Before tensile testing the specimens were carefully ground and polished. After mechanical cycling the gauges of the elongated specimens were cut and dilatometry, XRD and SEM studies were performed on unetched surfaces.

3. Experimental results and discussion

The loading-unloading curves of PM-MA specimens, up to a maximum strain of 4 %, are illustrated in Fig.2, together with their failure curve. As compared to typical slip induced plasticity of plain carbon steels, with elastic region, the deformation illustrated in Fig. 2(a) reveals plastic regions which are more rounded, being characteristic for transformation induced plasticity (TRIP) [10]. Unloading is accompanied by additional spring back which is the main characteristic of pseudoelasticity [11], However both TRIP and pseudoelasticity occurred only during first

loading-unloading cycle, in Fig.2(b) and (c) suggesting that stress induced martensitic transformation is the governing deformation mechanism only during first loading while slip becomes prominent during subsequent cycles. Fig.2(d) shows that PM-MA specimens are rather brittle since failure occurred at a strain of 5.5 %.

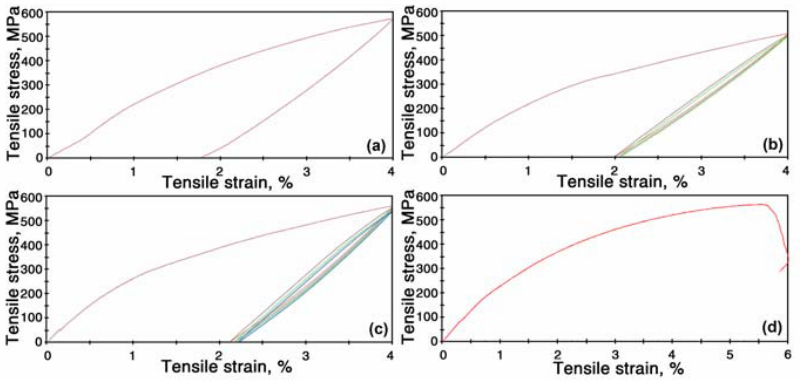

Fig.2: Tensile loading-unloading curves of PM-MA specimens: (a) 1 cycle to 4 %; (b) 3cycles to 4 %; (c) 5 cycles to 4 %; (d) failure curve.

The characteristic tensile loading-unloading curves of PM-Zn specimens are summarized in Fig.3, for 20, 40 and 100 cycles up to a maximum stress of 600 MPa.

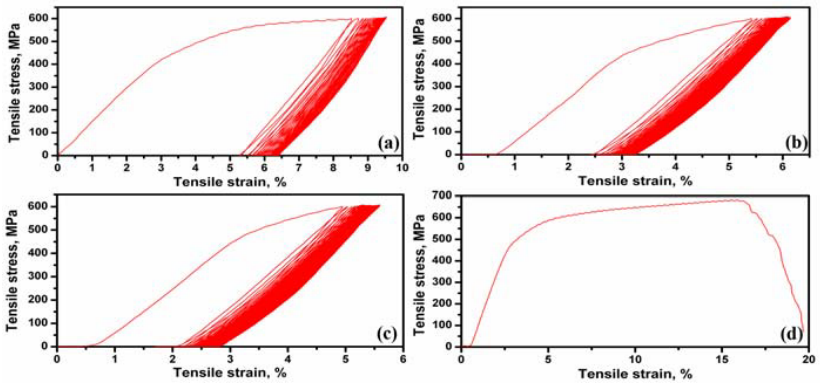

Fig.3 Tensile loading-unloading curves of PM-Zn specimens: (a) 20 cycles to 600 MPa; (b) 40cycles to 600 MPa; (c) 100 cycles to 600 MPa; (d) failure curve

As compared to PM-MA specimens, PM-Zn specimens did not experience TRIP behavior, preserved their pseudoelasticity and appear to be tougher, since they failed above 16 % strain. In order to reveal the changes induced by mechanical cycling on the closed loading-unloading loops, observed even after a few applied cycles, these loops were identified and isolated for every 10 cycles, up to 100. It was noticed that the loops preserved their shape and only the strain values increased with increasing the number of cycles.

The pseudoelasticity parameters were calculated for every 10 loading-unloading loops shown in Fig.3(c). These parameters are (i) of energetic nature: E_2 = unloading-released energy-proportional to the area under the unloading portion of the loop; E_1 = friction-dissipated energy-proportional to the area between loading and unloading portions of the loop and $\eta=E_2/(E_1+E_2)\times100$ = energy storage efficiency and (ii) of deformational nature: ε_t = total strain; ε_p = permanent strain and $(\varepsilon_t-\varepsilon_p)/\varepsilon_t\times100$ = strain recovery degree [11]. The evolutions of pseudoelasticity parameters as a function of the number of cycles are shown in Fig.4.

It is noticeable that unloading-released energy (E_2) tends to decrease, in Fig.4(a) while total and permanent strains tend to increase with increasing the number of mechanical cycles up to 100, in Fig.4(b). The relative decrease of unloading-released energy, after 100 cycles, has been 2.24 %. Since friction-dissipated energy (E_1) decreased less intensely, energy storage efficiency (η) experienced a slight increasing tendency, from approx. 92 to 94 %, after100 cycles. On the other hand, since permanent strain increased more than total strain, strain recovery degree, $(\varepsilon_t - \varepsilon_p)/\varepsilon_t \times 100$, decreased from approx. 61 % to about 46 %.

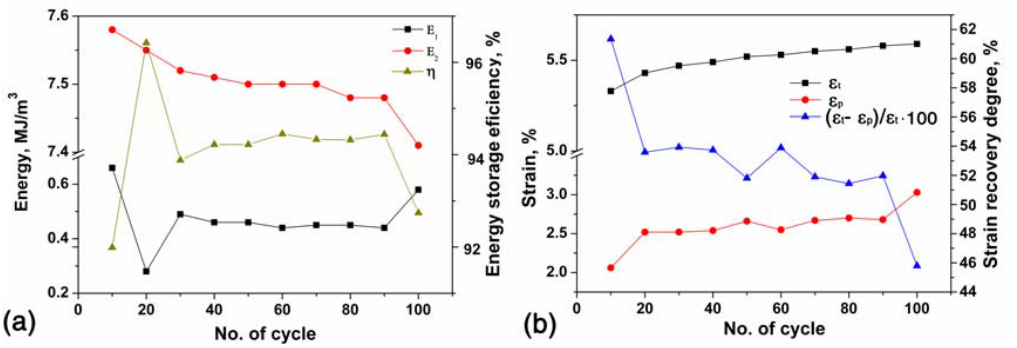

Fig.4: Evolution of pseudoelasticity parameters with the number of mechanical cycles, according to Fig.3(c): (a) energetic parameters; (b) deformational parameters (see text for details).

In order to reveal mechanical cycling effects on the thermomechanical response, the gauges of PM-MA specimens, which were mechanically cycled as in Fig.2, were analyzed by dilatometry. The variations with temperature of relative elongation, dL/L_0 and of thermal expansion coefficient, α are illustrated in Fig.5.

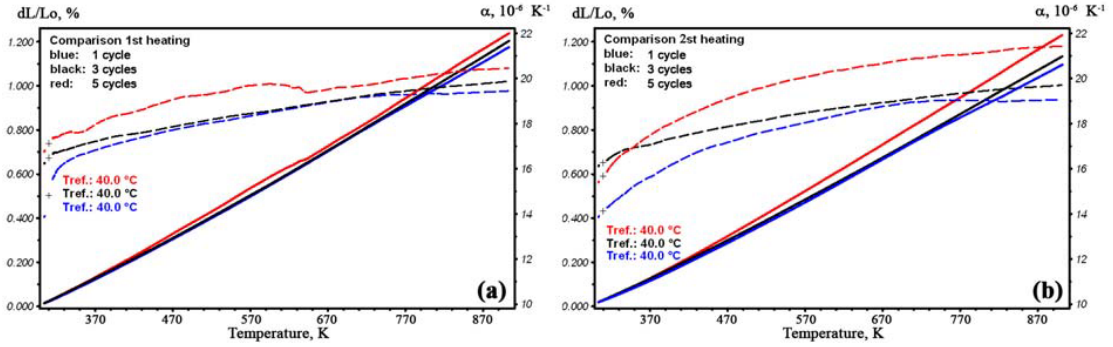

Fig.5: Evolution of thermomechanical responses of the gauges of specimens PM-MA, after being cycled according to Fig.2, revealed by the variations of relative elongation and thermal expansion coefficient with temperature, recorded by dilatometry: (a) during first heating; (b) during second heating.

The increase of the number of cycles has obviously enhanced relative elongation, the tendency being more prominent during second heating, in Fig.5(b). On the other hand, it is only during first heating cycle, in Fig.5(a), that a slight contraction occurred at approx. 630 K in the specimen subjected to 5 mechanical cycles. This solid state transition is accompanied by a more prominent decrease of thermal expansion coefficient. These results suggest that, in PM-MA specimens subjected to 5 mechanical cycles, a stress induced martensitic transformation occurred with low intensity. In order to confirm this assumption, structural analyses were performed by XRD and SEM.

The XRD patterns recorded on the gauges of PM-MA specimens, mechanically cycled as in Fig.2, are shown in Fig.6. Since these specimens proved to be rather brittle, the number of applicable mechanical cycles was low. Therefore these experiments aimed to reveal only the variation tendencies of PM-MA specimens during cycling.

The presence of only four diffraction maxima was revealed, among which three belong to γ (fcc) austenite, namely γ(111),γ(200) and γ(220), respectively. The fourth maxima was ascribed to the main diffraction peak of α' (bcc) martensite, α(110), considering that the spacings determined for $\alpha_{(110)}$, range between 0.20328 and 0.020362 nm, which are close enough to the value found in literature, $d_{\alpha(110)}$ = 0.02026 nm [12]. As previously reported, no ε (hcp) martensite was identified for this alloy composition which suggests that the low intensity slight solid state transition observed by dilatometry would simply correspond to the reversion to γ (fcc) austenite of α' (bcc) stress induced martensite, on heating [9].

A very similar phase structure was found in Fig.7 corresponding to PM-Zn specimens in initial state, Fig.7(a) and after 20 mechanical cycles, as shown in Fig.3(b)

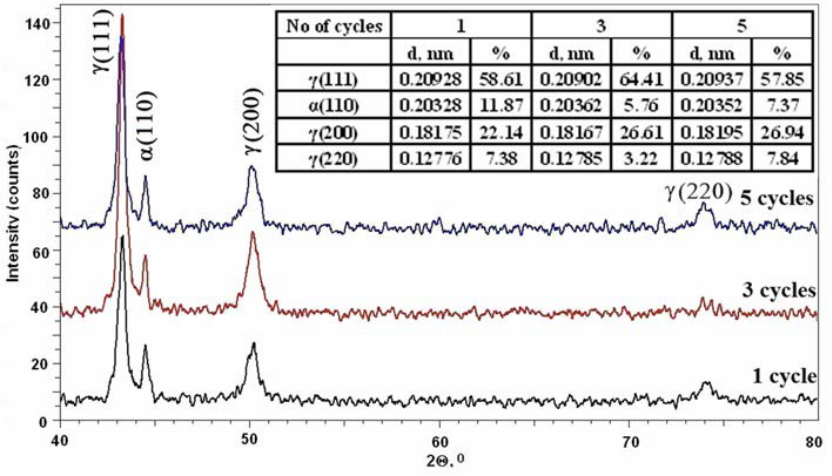

No of cycles	1		3		5	
	d, nm	%	d, nm	%	d, nm	%
γ(111)	0.20928	58.61	0.20902	64.41	0.20937	57.85
α(110)	0.20328	11.87	0.20362	5.76	0.20352	7.37
γ(200)	0.18175	22.14	0.18167	26.61	0.18195	26.94
γ(220)	0.12776	7.38	0.12785	3.22	0.12788	7.84

Fig.6: Mechanical cycling effects on the XRD patterns of the gauges of specimens PM-MA cycled as in Fig.2

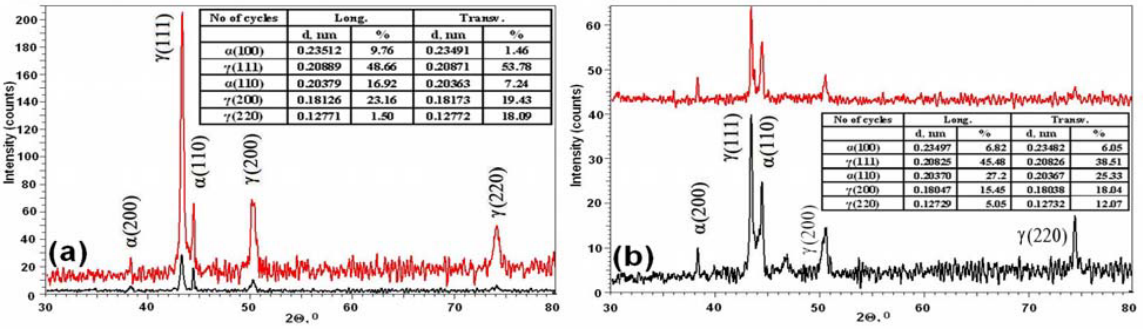

No of cycles	Long.		Transv.	
	d, nm	%	d, nm	%
α(100)	0.23512	9.76	0.23491	1.46
γ(111)	0.20889	48.66	0.20871	53.78
α(110)	0.20379	16.92	0.20363	7.24
γ(200)	0.18126	23.16	0.18173	19.43
γ(220)	0.12771	1.50	0.12772	18.09

No of cycles	Long.		Transv.	
	d, nm	%	d, nm	%
α(100)	0.23497	6.82	0.23482	6.05
γ(111)	0.20825	45.48	0.20826	38.51
α(110)	0.20370	27.2	0.20367	25.33
γ(200)	0.18047	15.45	0.18038	18.04
γ(220)	0.12729	5.05	0.12732	12.07

Fig.7: Mechanical cycling effects on the XRD patterns of the gauges of specimens PM-Zn, in parallel (Long.-upper, with red) and perpendicular position (Transv.-lower, with black) to X-ray beam: (a) initial; (b) after 20 cycles

In this case, 2Θ range was increased to 20-80^0 and the fifth peak was noticed which was ascribed to α(200). Due to hot rolling texture, marked differences of the phase amounts are noticeable in the XRD patterns corresponding to the two different orientations of the specimens, in respect to the X-ray beam, namely parallel (upper patterns, with red color) and perpendicular (lower patterns, with black color). Thus, it is obvious that a larger amount of α' martensite was oriented with its close packed planes parallel (approx. 27 %) than perpendicular (approx. 9 %) to rolling direction. The total amount of α' martensite increased after mechanical cycling, from less than 27% to about

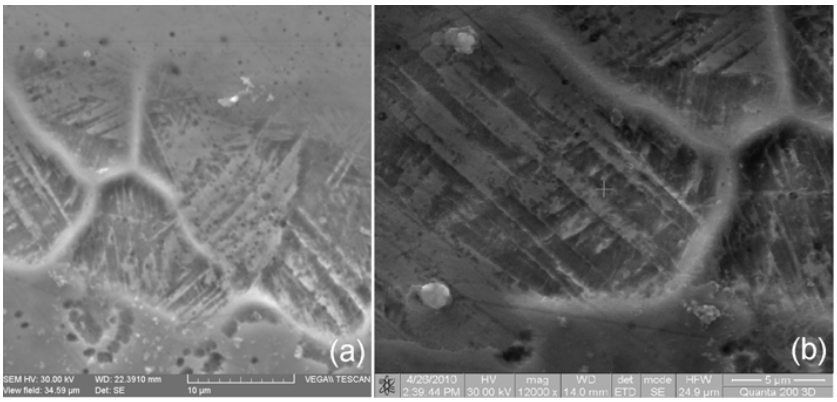

Fig.8: SEM micrographs revealing α' stress induced martensite on unetched surface of PM-Zn specimens subjected to 20 mechanical cycles: (a) general view of four adjacent grains; (b) detail of the lower left grain.

34 % for parallel position and from less than 9% to less than 32% for perpendicular position. It is obvious that the specimens sintered from commercial powders with zinc stearate binder contain more α' martensite than the specimens sintered from mechanically alloyed powders. In the XRD pattern recorded on transversal direction on the specimen subjected to 20 mechanical cycles, Fig.7(b), a low height additional peak occurred, around $2\theta=47^0$, which does not seem to belong to any of the previously observed phases and is less relevant for the present study.

Summarizing the above, it can be estimated that in PM-Zn specimens where zinc stearate was used as a binder, the stress induced formation of α' martensite can be associated with the disappearance of transformation induced plasticity and with the preservation of pseudoelastic character up to 100 cycles. On the other hand, mechanical cycling caused a decreasing tendency of α' martensite amount in PMMA specimens that do not have any binder. The presence of α' martensite was confirmed by SEM observations on the unetched surfaces of mechanically cycled specimens PM-Zn, as are illustrated in Fig.8. The surface relief characteristic to α' martensite is obvious in the high magnification detail of Fig.8(b).

4. Conclusions

The specimens of PM Fe-18Mn-3Si-7Cr-4Ni alloy, obtained both from commercial powders with zinc stearate binder (PM-Zn) and from mechanically alloyed powders (PM-MA), revealed transformation-induced plasticity during the first tensile loading and slip induced plasticity during subsequent ones and displayed pseudoelastic character during unloading. In the case of PM-Zn specimens the pseudoelastic character was only slightly diminished by mechanical cycling, since strain recovery degree decreased from approx. 61 % to about 46 %, yet energy storage efficiency remained above 92 %, after 100 cycles. In the case of mechanically cycled PM-MA specimens a low intensity solid state transition occurred during first heating, which was ascribed to thermally-induced reversion to austenite of α' stress-induced martensite. The amount of α' martensite increased with the number of mechanical cycles, mostly along parallel directions to hot rolling one and its presence was ascertained by XRD and SEM.

Acknowledgements

This work was financially supported by UEFISCU by means of the research grant PN II-ID 301-PCE-2007-1, contract no. 279/01.10.2007. B.P. acknowledges the funding offered by EURODOC program. Special thanks are brought to Dr. Markus Meyer from Netzsch for the support in dilatometric study.

References

[1] J. L. Proft, T. W. Duerig, in T. W. Duerig, K. N. Melton, D. Stöckel, C. M. Wayman (eds.), Engineering Aspects of Shape Memory Alloys, Butterworth-Heinemann, 1990, 115
[2] S. Kajiwara, A.L. Baruj, T. Kikuchi, N. Shinya, Proc. of SPIE Vol. 5053(2003)251
[3] T. Maruyama, T. Kurita, S. Kozaki, K. Andou, S. Farjami, H. Kubo, Mater. Sci. Technol. 16(2000 612
[4] H. Otsuka, H. Yamada, T. Maruyama, H.; Tanahashi, S.; Matsuda, M. Murakami, ISIJ Int, 30(1990)674
[5] Y. Moriya, H. Kimura, S. Ishizaki, S. Hashizume, S. Suzuki, H. Suzuki and T. Sampei, J Phys III, Vol. 1, novembre (1991)C4-433
[6] T. Maki, in K. Otsuka and C.M. Wayman (eds.), Shape Memory Materials, edited, Cambridge, University Press, 1998, 133
[7] L. Bracke, G. Mertens, J. Penning, B.C. De Cooman, M. Liebeherr, N. Akdut, Metall. Mater. Trans. A, 37A, February, (2006)307
[8] B. Dubois, Trait. Thermique, 234 (1990) 27
[9] L. G. Bujoreanu , S. Stanciu, B. Özkal, R. I. Comăneci, M. Meyer, Proc. ESOMAT 2009,05003(2009)
[10] N. Gu, C. Lin, X. Song, H. Peng, F. Yin, Q. Liu, Mater. Sci Forum 327-328 (2000)231
[11] T.W. Duerig, R. Zadno, in W. Duerig, K. N. Melton, D. Stöckel, C. M. Wayman (eds.), Engineering Aspects of Shape Memory Alloys, Butterworth-Heinemann, 1990, 369
[12] K.M. Mostafa, J. De Baerdemaeker, N. Van Caenegem, D. Segers, and Y. Houbaert, J Mater Perform 18(5-6) (2009) 575